Applied Physics Letters

Super-oscillatory optical needle

Cite as: Appl. Phys. Lett. **102**, 031108 (2013); https://doi.org/10.1063/1.4774385
Submitted: 01 November 2012 . Accepted: 20 December 2012 . Published Online: 23 January 2013

Edward T. F. Rogers, Salvatore Savo, Jari Lindberg, Tapashree Roy, Mark R. Dennis, and Nikolay I. Zheludev

View Online Export Citation CrossMark

ARTICLES YOU MAY BE INTERESTED IN

Point spread function of the optical needle super-oscillatory lens
Applied Physics Letters **104**, 231109 (2014); https://doi.org/10.1063/1.4882246

Focusing of light by a nanohole array
Applied Physics Letters **90**, 091119 (2007); https://doi.org/10.1063/1.2710775

Far field subwavelength focusing using optical eigenmodes
Applied Physics Letters **98**, 181109 (2011); https://doi.org/10.1063/1.3587636

© 2013 American Institute of Physics.

AIP Publishing

Super-oscillatory optical needle

Edward T. F. Rogers,[1] Salvatore Savo,[1] Jari Lindberg,[2] Tapashree Roy,[1] Mark R. Dennis,[2] and Nikolay I. Zheludev[1,3]
[1]*Optoelectronics Research Centre and Centre for Photonic Metamaterials, University of Southampton, University Road, Southampton SO17 1BJ, United Kingdom*
[2]*H. H. Wills Physics Laboratory, University of Bristol, Bristol BS8 1TL, United Kingdom*
[3]*Centre for Disruptive Photonic Technologies, Nanyang Technological University, Singapore*

(Received 1 November 2012; accepted 20 December 2012; published online 23 January 2013)

Super-oscillatory optical lenses have recently been shown to achieve subwavelength focusing and have been used for super-resolution imaging. However, the subwavelength hotspots created by these lenses are always accompanied by sidebands containing a significant fraction of the optical energy and are highly localised in the axial direction. Here, we report a class of super-oscillatory lenses that form extended subwavelength optical needles on a 15λ field of view. © *2013 American Institute of Physics*. [http://dx.doi.org/10.1063/1.4774385]

The Arago spot[1,2] excited great controversy when first proposed and was one of the early proofs of the wave theory of light. In this letter, we will show that this 200-yr-old phenomenon still has applications at the cutting edge of nanophotonics.

Super-oscillatory lenses (SOLs) are a promising technology for subwavelength focusing[3] and imaging[4,5] beyond the near field, but use of the hotspots in some applications is limited by the presence of sidebands in the region of the spot. Following from the principle of super-oscillation,[6,7] these lenses focus light into subwavelength spots. Other focusing methods similarly inspired by super-oscillation include a mask with variable attenuation and retardation[8] or by using precisely engineered arrangements of waveguides[9–11] or microwave antennas,[12,13] but all these methods suffer from sidebands of significant intensity near the focal spot.[6,14] Near field approaches to focusing[15–19] can produce subwavelength spots without sidebands, but they are limited in many applications as the focal spot is in the near field of the "lens." While imaging in the presence of sidebands has been successfully demonstrated, these sidebands restrict the use of these spots in other applications. For example, in direct write lithography, it would be impossible to use the hotspot to write a subwavelength feature in a photoresist without simultaneously exposing the resist illuminated by the sidebands.

Here, we propose and demonstrate a class of SOLs, which we term optical needle SOLs (ONSOLs), in which the sidebands are moved far from the focal spot. These lenses also produce an extended focal spot in the axial direction, in contrast to standard SOLs which produce one or more axially localised spots. These optical needles are ideal for imaging or writing of planar structures, although they reduce axial resolution in 3D imaging applications.

It should be noted that the optical needles described here are distinct from those formed by longitudinal polarisation[20–22] as they form a subwavelength needle from a linearly polarised input beam, allowing much easier realization and a wide range of applications. For example, ONSOLs would be well suited to selectively coupling light into an array of waveguides on a nanophotonic chip. Each transverse slice of the optical needle has radial oscillations similar to a non-diffracting Bessel beam,[23,24] although the pattern changes on propagation, while retaining its needle-like character. The ONSOL also forms the needle from a complex interference of beams with a large range of k vectors, rather than the very narrow range in a Bessel beam.

Below we discuss the design of the ONSOL and compare its focusing performance to that of a standard SOL and a simple disc.

The principle of operation of a ONSOL is the same as that of a standard SOL:[5] the careful design of the lens diffracts an incident plane light wave so that it interferes constructively at the focal spot. The crucial difference in a ONSOL is that the central region of the lens is obscured by a stop, forming a shadow region in which the focus is formed (Fig. 1).

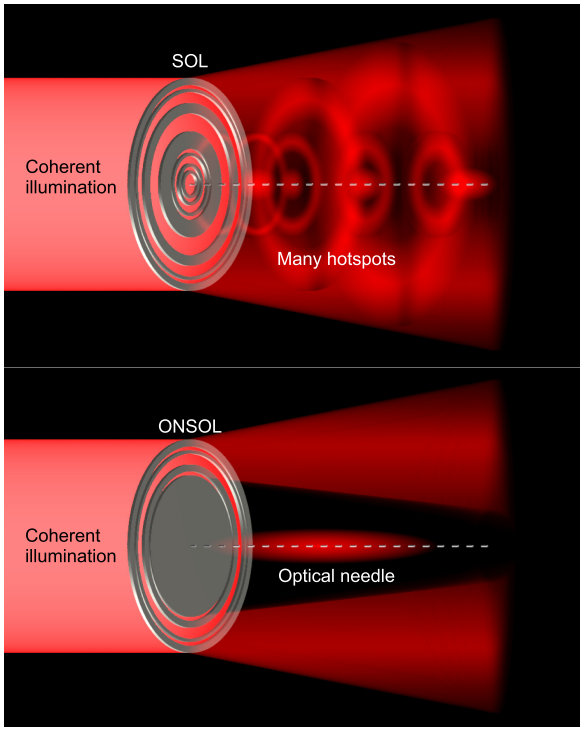

FIG. 1. Comparison of SOL and ONSOL. The SOL produces a complex pattern of spots and sidebands at different distances for the lens. The ONSOL produces a much simpler pattern with a subwavelength needle on the optical axis and sidebands far from the axis.

 © 2013 American Institute of Physics

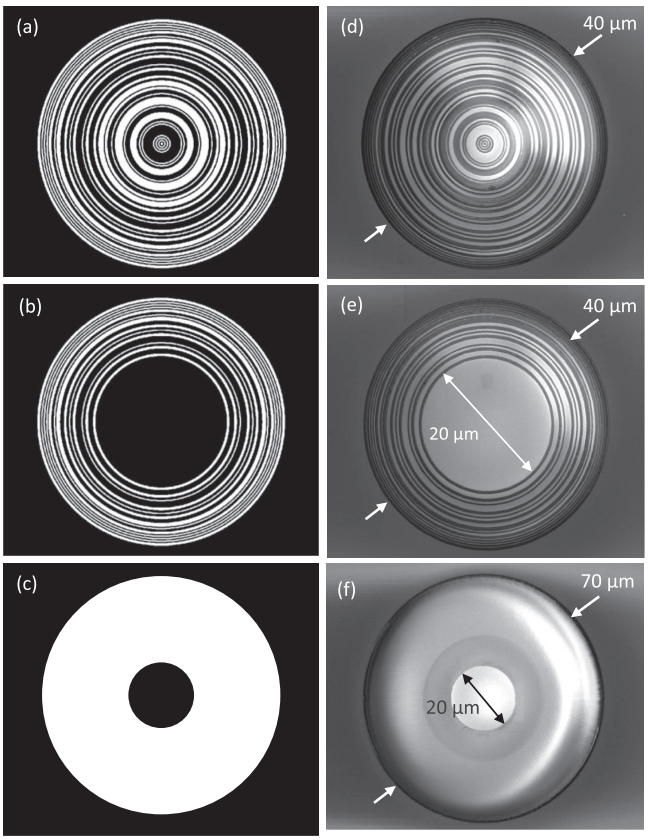

FIG. 2. Designs ((a)–(c)) and SEM images ((d)–(f)) of the of the lenses. (a) and (d) SOL, (b) and (e) ONSOL with 20 μm diameter opaque region, (c) and (f) control sample; 20 μm diameter Au disk in a 70 μm diameter transparent region.

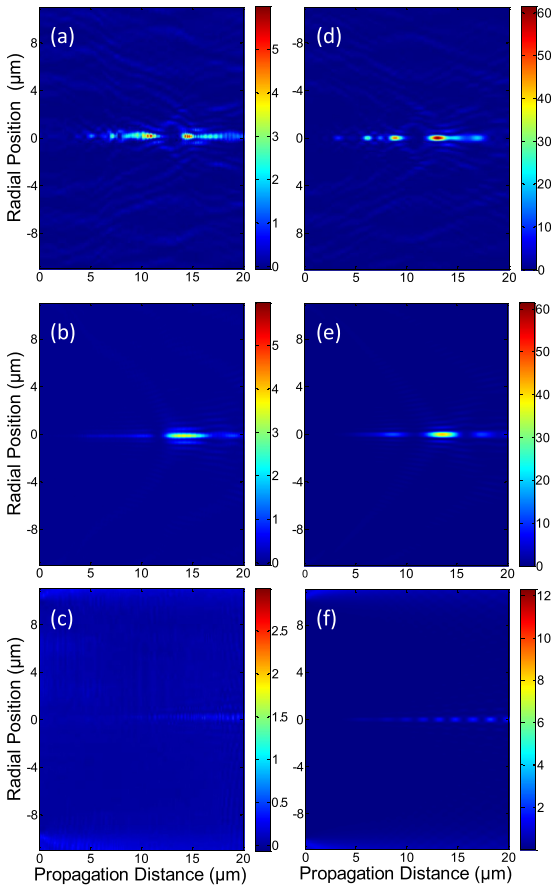

FIG. 3. Experimental ((a)–(c)) and simulated ((d) and (e)) intensity of the lens interference patterns. (a) and (d) SOL, (b) and (e) ONSOL with 20 μm diameter opaque region, (c) and (f) disc control sample. The colour scale in plots (c) and (f) has been adjusted to improve the visibility of the very low intensity spots.

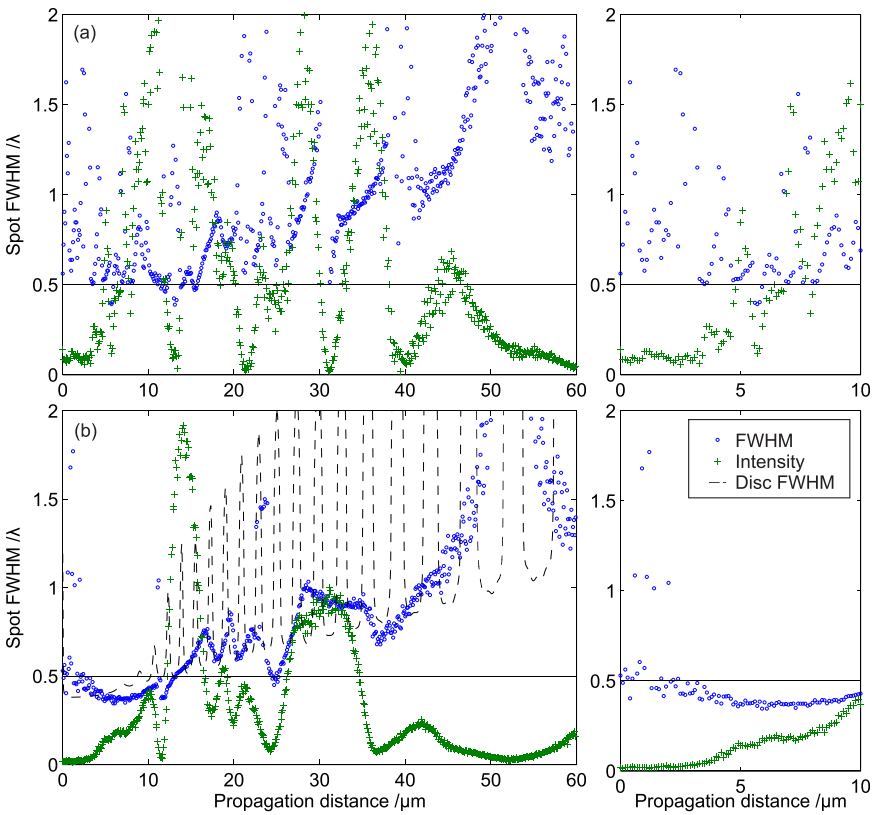

FIG. 4. Distribution of FWHM and axial intensity (in arbitrary units) with propagation distance away from the lens for (a) the SOL, (b) the ONSOL; each figure on the right hand side shows the corresponding zoomed-in view from 0 to 10 μm. The simulated FWHM of the disc spot is shown in (b) by the dashed line.

Figs. 2(a) and 2(d) show a standard SOL that creates multiple focal spots, while Figs. 2(b) and 2(e) show the same lens converted to a darkfield configuration, by inclusion of a 20 μm diameter opaque circle at the centre of the lens. The design of the two lenses is otherwise identical. The lenses are manufactured by focused ion beam (FIB) milling of a 100 nm thick gold film deposited on a silica substrate. We compare the performance of the two lenses to that of a simple gold disc (Figs. 2(c) and 2(f), diameter 20 μm) formed in the same gold film with an unstructured transparent region around it.

To experimentally characterise the focusing performance of the masks shown in Fig. 2, they are illuminated by a collimated laser beam with wavelength 640 nm. A conventional microscope with high NA objective (Nikon CFI LU Plan Apo EPI 150X, NA = 0.95) is used to capture the diffraction pattern generated by the mask at various distances away from the surface. Since the subwavelength focal spots are formed by interference of propagating waves, they can be accurately imaged through a conventional microscope.

Figures 3(a)–3(c) show the experimental evolution of the focal spots with distance from the lens. Comparison with simulations using the scalar angular spectrum method (Figures 3(d)–3(f)) shows excellent agreement, demonstrating that the focusing effect does not rely on the light's vectorial nature and indicating the adequacy of the scalar theory for the focusing effect we describe. In the case of the standard SOL (Figs. 3(a) and 3(d)), several focal spots are formed at different distances from the lens. However, the ONSOL forms an $\approx 7\mu$m long optical needle, starting 4 μm from the lens. The control sample forms a series of spots that are a factor of five lower in intensity than those formed by the SOLs. These are manifestations of the well-known Arago spot, formed in the shadow of a circular obstruction.

Figure 4 shows the distribution of the measured full width at half maximum (FWHM) of the hotspots generated by each of the three structures. For a conventional SOL, the smallest spot (0.35λ) is found at 5.7 μm (shown in Fig. 5(a)). No subwavelength spots are formed by the SOL beyond 15 μm. For the ONSOL, the smallest spot is found at 5.9 μm (Fig. 5(b)). Though this is larger (0.42λ) than that in the case of the SOL, it has the advantage of being isolated from any significantly intense sidebands as shown in Fig. 5(d). The FWHM distribution of the ONSOL (Fig. 4(b)) shows that from about 4 μm to 10 μm, a needle is formed with a constant subwavelength width. The intensity of this needle is monotonically increasing and varies by less than a factor of 2 between 5 μm and 9 μm, more than 6λ. No such needle is seen in the case of the SOL. Interestingly, beyond z = 40 μm, the FWHM distribution looks similar for both the SOL and the ONSOL. The dashed line in Fig. 4(b) shows the simulated FWHM distribution for Arago spots formed by the 20 μm gold disk. The subwavelength spots seen near the gold disc in the simulation are of such low intensity that they cannot be measured experimentally.

Fig. 6 shows the effect of a change of blocking region diameter on the optical needle without varying the rest of the ONSOL. As might be expected from a consideration of simple diffraction effects, the main effect of increasing the size of the blocking region is to move the needle away from the ONSOL and to increase the size of the field of view around the needle. The intensity of the needle also reduces, primarily as a result of the lower overall transmission of the masks with larger blocking regions. For the diameter of 20 μm used in the experiments, we achieve a reasonable compromise of needle intensity and length

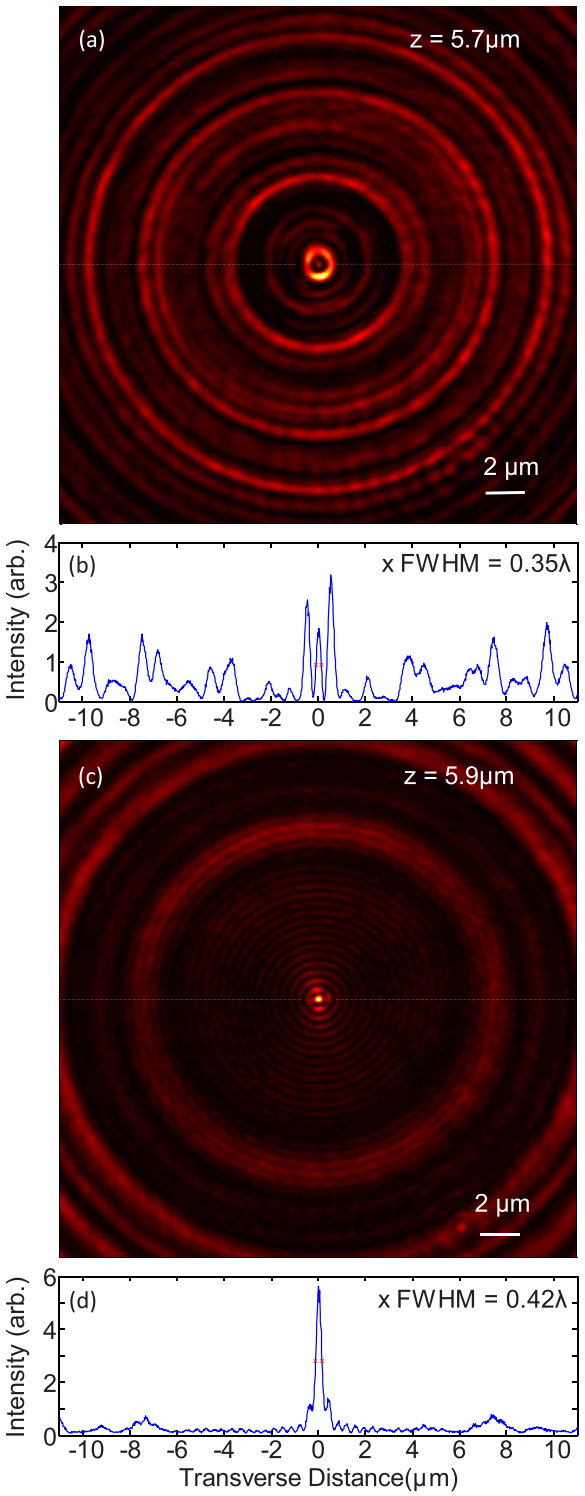

FIG. 5. Focal spots at (a) $z = 5.7\,\mu$m for the SOL and at (c) $z = 5.9\,\mu$m for the ONSOL. (b) and (d) show intensity profiles through the lines in (a) and (c), respectively.

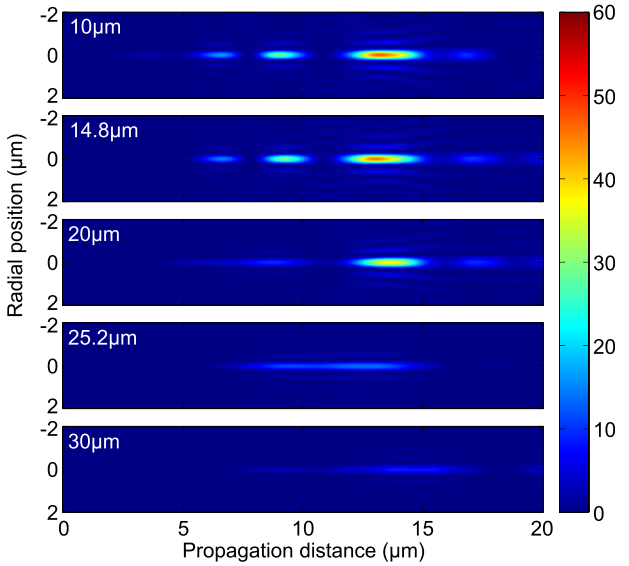

FIG. 6. Simulated optical needles formed by ONSOLs with various diameters of the blocking region. The length of the needle increases with the diameter of the blocking region and the needle moves further from the ONSOL, but the intensity of the needle reduces.

while forming the needle far enough from the mask to be technologically useful.

In conclusion, we have demonstrated focusing into isolated subwavelength spots beyond the near field and the creation of an (11λ) long subwavelength optical needle. The easy-to-manufacture ONSOL will have applications in many areas of nanophotonics such as super-resolution imaging and nanofabrication with light.

This work was funded by the United Kingdom Engineering and Physical Sciences Research Council, grant number EP/F040644/1, and the Advanced Optics in Engineering Programme, A*STAR, Singapore.

[1]A. J. Fresnel, *Œuvres complètes d'Augustin Fresnel: Théorie de la lumière* (Imprimerie impériale, 1866).
[2]F. L. Pedrotti and L. S. Pedrotti, *Intoduction to Optics*, 2nd ed. (Prentice-Hall, New Jersey, USA, 1993).
[3]J. Baumgartl, S. Kosmeier, M. Mazilu, E. T. F. Rogers, N. I. Zheludev, and K. Dholakia, Appl. Phys. Lett. **98**, 181109 (2011).
[4]S. Kosmeier, M. Mazilu, J. Baumgartl, and K. Dholakia, J. Opt. **13**, 105707 (2011).
[5]E. T. F. Rogers, J. Lindberg, T. Roy, S. Savo, J. E. Chad, M. R. Dennis, and N. I. Zheludev, Nature Mater. **11**, 432 (2012).
[6]G. Toraldo di Francia, Nuovo Cimento **9**(Suppl.), 426 (1952).
[7]M. V. Berry and S. Popescu, J. Phys. A: Math. Gen. **39**, 6965 (2006).
[8]F. M. Huang and N. I. Zheludev, Nano Lett. **9**, 1249 (2009).
[9]X. Wang, J. Fu, X. Liu, and L.-M. Tong, J. Opt. Soc. Am. A **26**, 1827 (2009).
[10]R. Gordon, Phys. Rev. Lett. **102**, 207402 (2009).
[11]D. Choi, Y. Lim, S. Roh, I.-M. Lee, J. Jung, and B. Lee, Appl. Opt. **49**, A30 (2010).
[12]A. Wong and G. Eleftheriades, IEEE Antennas Wireless Propag. Lett. **9**, 315 (2010).
[13]A. Wong and G. Eleftheriades, IEEE Trans. Antennas Propag. **59**, 4766 (2011).
[14]Z. S. Hegedus and V. Sarafis, J. Opt. Soc. Am. A **3**, 1892 (1986).
[15]R. J. Blaikie and D. O. S. Melville, J. Opt. A, Pure Appl. Opt. **7**, S176 (2005).
[16]N. Fang, H. Lee, C. Sun, and X. Zhang, Science **308**, 534 (2005).
[17]I. I. Smolyaninov, Y.-J. Hung, and C. C. Davis, Science **315**, 1699 (2007).
[18]A. Salandrino and N. Engheta, Phys. Rev. B **74**, 075103 (2006).
[19]B. Hecht, B. Sick, U. Wild, V. Deckert, R. Zenobi, O. Martin, and D. Pohl, J Chem. Phys. **112**, 7761 (2000).
[20]H. Wang, L. Shi, B. Lukyanchuk, C. Sheppard, and C. T. Chong, Nat. Photonics **2**, 501 (2008).
[21]J. Wang, W. Chen, and Q. Zhan, Opt. Express **18**, 21965 (2010).
[22]C.-C. Fang, T.-D. Cheng, J.-T. Yeh, K.-C. Wu, and C.-K. Lee, Opt. Express **17**, 13646 (2009).
[23]J. Durnin, J. J. Miceli, and J. H. Eberly, Phys. Rev. Lett. **58**, 1499 (1987).
[24]T. Čižmár and K. Dholakia, Opt. Express **17**, 15558 (2009).